

Differential Conductance and Quantum Interference in Kondo Systems

Jeremy Figgins and Dirk K. Morr

Department of Physics, University of Illinois at Chicago, Chicago, Illinois 60607, USA

(Received 22 January 2010; published 6 May 2010)

We present a large- N theory for the differential conductance, dI/dV , in Kondo systems measured via scanning tunneling spectroscopy. We demonstrate that quantum interference between tunneling processes into the conduction band and into the magnetic f -electron states is crucial in determining the experimental Fano line shape of dI/dV . This allows one to uniquely extract the Kondo coupling and the ratio of the tunneling amplitudes from the experimental dI/dV curve. Finally, we show that dI/dV directly reflects the strength of the antiferromagnetic interaction in Kondo lattice systems.

DOI: 10.1103/PhysRevLett.104.187202

PACS numbers: 75.20.Hr, 71.27.+a, 72.15.Qm, 74.55.+v

Recent progress in scanning tunneling spectroscopy (STS) techniques has made it possible for the first time to measure the differential conductance, dI/dV , in heavy-fermion compounds [1]. These materials, whose essential ingredient is a (Kondo) lattice of magnetic moments that is coupled to a conduction band [2], exhibit a variety of puzzling phenomena, ranging from non-Fermi-liquid behavior to unconventional superconductivity [3]. Their microscopic origin likely lies in the competition between an antiferromagnetic ordering of the magnetic moments and their screening by conduction electrons [2], though no theoretical consensus has emerged as yet [4]. STS experiments, by providing insight into the local electronic structure [1] of heavy-fermion materials, might hold the key to understanding their complex properties. The theoretical challenge in the interpretation of the differential conductance in Kondo lattice systems [5,6], and around single Kondo impurities [7–13], arises from the quantum interference between electrons tunneling from the STS tip into the conduction band and into the magnetic f -electron states. While dI/dV for a single Kondo impurity has been successfully described [7–11] using a phenomenological form derived by Fano [14], a microscopic understanding of how the interplay between the strength of the Kondo coupling, the interaction between the magnetic moments, the electronic structure of the screening conduction band, and quantum interference determines the dI/dV line shape is still lacking.

In this Letter, we address this issue within the framework of a large- N theory and identify the microscopic origin for the form of dI/dV not only around single Kondo impurities but also in Kondo lattice systems. We show that the line shape and the spatial dependence of dI/dV sensitively depend on the particle-hole asymmetry of the (screening) conduction band, as well as the quantum interference between the two tunneling paths. For a single Kondo impurity, this sensitivity allows one to uniquely extract the Kondo coupling, J ; the ratio of the tunneling amplitudes into the conduction band and magnetic f -electron states, t_c and t_f , respectively; and the impurity spin from the experimental STS data. In addition, for a Kondo lattice,

the dI/dV line shape provides insight into the strength of the interaction between the magnetic moments. Because of quantum interference effects, the differential conductance is qualitatively different from the local density of states (LDOS) of either the conduction band or the f -electron states. However, once the pertinent parameters are extracted from a theoretical fit to dI/dV , we can predict the frequency and spatial dependence of the LDOS for both bands, as well as the electronic correlations between them, thus providing important insight into the complex electronic structure of Kondo systems.

We begin by considering the form of dI/dV in a system containing a single Kondo impurity with Hamiltonian

$$\mathcal{H} = - \sum_{\mathbf{r}, \mathbf{r}', \sigma} t_{\mathbf{r}\mathbf{r}'} c_{\mathbf{r}, \sigma}^\dagger c_{\mathbf{r}', \sigma} + J \mathbf{S}_{\mathbf{R}}^K \cdot \mathbf{s}_{\mathbf{R}}^c, \quad (1)$$

where $t_{\mathbf{r}\mathbf{r}'}$ is the fermionic hopping element between sites \mathbf{r} and \mathbf{r}' of the conduction band, $c_{\mathbf{r}, \sigma}^\dagger$ ($c_{\mathbf{r}, \sigma}$) creates (annihilates) a fermion with spin σ at site \mathbf{r} , and the sum runs over all sites of the conduction band. $\mathbf{S}_{\mathbf{R}}^K$ and $\mathbf{s}_{\mathbf{R}}^c$ are the spin operators of the Kondo impurity and the conduction electrons at site \mathbf{R} , respectively, and $J > 0$ is the Kondo coupling. To describe the Kondo screening of the magnetic impurity, we employ a large- N expansion [15–21] whose general validity has been established previously [16,19]. Here, $\mathbf{S}_{\mathbf{R}}^K$ is generalized to $SU(N)$ and represented via Abrikosov pseudofermions f_m^\dagger, f_m which obey the constraint $\sum_{m=1\dots N} f_m^\dagger f_m = 1$ where $N = 2S + 1$ is the spin degeneracy of the magnetic impurity. This constraint is enforced by means of a Lagrange multiplier ε_f , while the exchange interaction in Eq. (1) is decoupled via a hybridization field, s . For fixed J , we then obtain ε_f and s on the saddle point level by minimizing the effective action [16]. Finally, the tunneling process into a conduction electron state at \mathbf{r} and the f -electron state at \mathbf{R} , as schematically shown in Fig. 1, is described by

$$\mathcal{H}_T = \sum_{\sigma} t_c c_{\mathbf{r}, \sigma}^\dagger d_{\sigma} + t_f f_{\mathbf{R}, \sigma}^\dagger d_{\sigma} + \text{H.c.}, \quad (2)$$

where d_{σ} destroys a fermion in the STS tip. The total

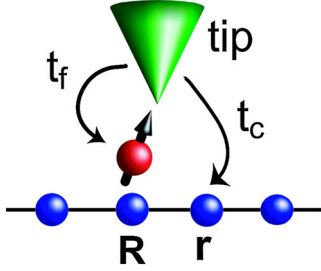


FIG. 1 (color online). Tunneling paths into the conduction and f -electron states with amplitudes t_c and t_f , respectively.

current flowing from the tip into the systems is [22]

$$I(V) = -\frac{e}{\hbar} \text{Re} \int_0^V \frac{d\omega}{2\pi} [t_c \hat{G}_{12}^K(\omega) + t_f \hat{G}_{13}^K(\omega)], \quad (3)$$

with the full Keldysh Green's function matrix given by

$$\begin{aligned} \hat{G}^K(\omega) &= [\hat{1} - \hat{g}^r(\omega)\hat{t}]^{-1} \hat{f}_0(\omega) [\hat{1} - \hat{t}\hat{g}^a(\omega)]^{-1}; \\ \hat{f}_0(\omega) &= 2i[1 - 2\hat{n}_F(\omega)] \text{Im}[\hat{g}^r(\omega)]; \\ \hat{g}^r(\omega) &= \begin{pmatrix} g_t^r(\omega) & 0 & 0 \\ 0 & g_{cc}^r(\mathbf{r}, \mathbf{r}, \omega) & g_{cf}^r(\mathbf{r}, \mathbf{R}, \omega) \\ 0 & g_{fc}^r(\mathbf{R}, \mathbf{r}, \omega) & g_{ff}^r(\mathbf{R}, \mathbf{R}, \omega) \end{pmatrix}. \end{aligned} \quad (4)$$

Here, \hat{t} is the symmetric hopping matrix with nonzero elements $\hat{t}_{12} = t_c$, $\hat{t}_{13} = t_f$. \hat{n}_F is diagonal containing the Fermi-distribution functions of the tip, f - and c -electron states. g_t^r is the retarded Green's function of the tip, and $g_{\alpha\beta}^r(\mathbf{r}', \mathbf{r}, \tau) = -\langle T_\tau \alpha_{\mathbf{r}'}(\tau) \beta_{\mathbf{r}}^\dagger(0) \rangle$ ($\alpha, \beta = c, f$) describes the many-body effects arising from the hybridization of the conduction band with the f -electron level, and the concomitant screening of the magnetic moment, with

$$\begin{aligned} g_{ff}^r(\mathbf{R}, \mathbf{R}, \omega) &= [\omega - \varepsilon_f - s^2 g_0^r(\mathbf{R}, \mathbf{R}, \omega)]^{-1}; \\ g_{cc}^r(\mathbf{r}, \mathbf{r}, \omega) &= g_0^r(\mathbf{r}, \mathbf{r}, \omega) \\ &\quad + g_0^r(\mathbf{r}, \mathbf{R}, \omega) s g_{ff}^r(\mathbf{R}, \mathbf{R}, \omega) s g_0^r(\mathbf{R}, \mathbf{r}, \omega); \\ g_{cf}^r(\mathbf{r}, \mathbf{R}, \omega) &= g_0^r(\mathbf{r}, \mathbf{R}, \omega) s g_{ff}^r(\mathbf{R}, \mathbf{R}, \omega), \end{aligned} \quad (5)$$

where g_0^r is the retarded Green's function of the unhybridized conduction electron band.

While the results shown below are obtained from Eq. (3) via differentiation, it is instructive to consider the leading order contributions to dI/dV in the weak-tunneling limit, $t_c, t_f \rightarrow 0$, given by

$$\begin{aligned} \frac{dI(V)}{dV} &= \frac{2\pi e}{\hbar} N_t [t_c^2 N_c(\mathbf{r}, V) + t_f^2 N_f(\mathbf{R}, V) \\ &\quad + 2t_c t_f N_{cf}(\mathbf{r}, \mathbf{R}, V)] \end{aligned} \quad (6)$$

with N_t , N_c , and N_f being the density of states of the tip, conduction, and f -electron states, respectively, and $N_{cf} = -\text{Im}g_{cf}^r/\pi$. The last term in Eq. (6) describes quantum interference processes between the two tunneling paths,

which, as we show below, are crucial in determining the line shape of the differential conductance.

In Fig. 2(a) we present the experimental dI/dV data of Ref. [11] for a tip positioned above a Co atom on a Au(111) surface together with a theoretical fit obtained from Eq. (3). Here, tunneling into the conduction band involves only the state at \mathbf{R} , i.e., $\mathbf{r} = \mathbf{R}$. The peak and dip in dI/dV are a direct signature of the hybridization between the conduction band and the f -electron state of the Kondo impurity and are commonly referred to as the Kondo resonance. As input parameters, we took the screening conduction band to be given by the Au(111) surface states possessing a triangular lattice structure with $t = 1.3$ eV and $\mu = -7.34$ eV [23], and used $N = 4$ as required for the description of the spin 3/2 of Co. The theoretical dI/dV curve is then solely determined by J and t_f/t_c , which control the width of the dip and the asymmetry of dI/dV , respectively. By performing an extensive survey, we found that there exists a unique set of parameters, $J = 1.39$ eV and $t_f/t_c = 0.0066$, that yield the very good quantitative agreement between the theoretical and experimental data shown in Fig. 2(a). While the STS tip is positioned above the Co atom, t_f/t_c is small, likely reflect-

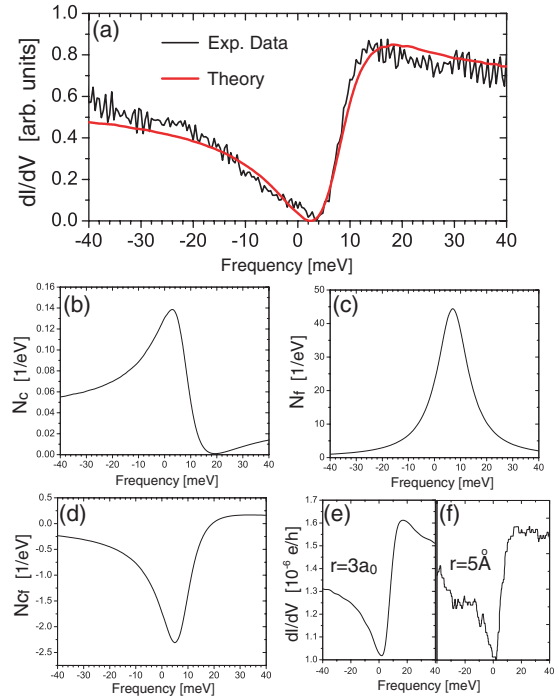


FIG. 2 (color online). (a) Experimental dI/dV curve of Ref. [11] at the site of a Co atom on a Au(111) surface together with a theoretical fit from Eq. (3) with $N = 4$, $t_f/t_c = 0.066$, $t_c = 1$ meV, $N_t = 1/\text{eV}$, and $J = 1.39$ eV yielding $s = 0.25$ eV, and $\varepsilon_f = 19$ meV. A constant background was subtracted from the experimental data. (b) Conduction electron LDOS, $N_c(\omega)$, (c) f -electron LDOS $N_f(\omega)$, and (d) $N_{cf}(\omega)$ at \mathbf{R} . (e) dI/dV at a distance of $r = 3a_0$ from the Co atom for $t_f = 0$. Parameters in (b)–(e) are the same as in (a). (f) Experimental dI/dV curve of Ref. [7] at $r = 5 \text{ \AA}$ from the Co atom.

ing the suppression of the tunneling process into the f -electron state by Coulomb effects. Moreover, using the value of J obtained from the fit, we computed the LDOS of the conduction and f -electron states, shown in Figs. 2(b) and 2(c), respectively, as well as N_{cf} [see Fig. 2(d)], which reflects the electronic correlations between the two bands. The fact that the line shape of the conduction band LDOS is qualitatively different from that of dI/dV demonstrates the importance of a second tunneling path and the resulting quantum interference in determining the latter. This conclusion is in direct contrast to the assumption of a single tunneling path made in Ref. [9]. Moreover, as the STS tip is moved away from the Co atom, direct tunneling into the f -electron state becomes suppressed and $t_f \rightarrow 0$ [10,13]. The theoretical dI/dV curve at a distance of $r = 3a_0$ from the Co atom, shown in Fig. 2(e), was therefore obtained with $t_f = 0$. Note that while $t_f = 0$, the asymmetry of dI/dV is now the same as that at the site of the Co atom, and qualitatively agrees with the experimental dI/dV curve at $r = 5 \text{ \AA}$ [7] shown in Fig. 2(f), demonstrating the consistency of our approach. A more quantitative fit would require an extensive spatial survey of dI/dV away from the Co atom. Finally we note that the good theoretical fit in Fig. 2(a) uniquely requires $N = 4$, consistent with the spin 3/2 of Co. Indeed, for $N = 2$, corresponding to $S = 1/2$, no fit to the experimental data can be obtained. In particular, while for $N = 2$ one can find a set of J and t_f/t_c that yields the overall asymmetry of the experimental dI/dV curve, the resulting theoretical curve is shifted to negative energies by about 5 meV (in comparison to the one for $N = 4$), thus clearly distinguishing the $N = 2$ and $N = 4$ cases [see, e.g., Fig. 3(d)]. This demonstrates that dI/dV directly reflects the spin of the screened magnetic moment.

The asymmetry of the dI/dV line shape is determined by two microscopic properties: the particle-hole asymmetry of the screening conduction band, and the ratio of the tunneling amplitudes, t_f/t_c . To demonstrate this dependence, we present in Fig. 3 the evolution of dI/dV with increasing ratio t_f/t_c . To contrast and complement the results shown in Fig. 2, we take $N = 2$, corresponding to a spin-1/2 moment, and consider a conduction band on a square lattice with $t = 0.5E_0$ and $\mu = -1.809E_0$. The resulting circular Fermi surface with Fermi wavelength $\lambda_F = 10a_0$ is representative of the Au(111) and Cu(111) surface states employed in Refs. [7,11,12]. For $t_f = 0$ [solid line in Fig. 3(a)], dI/dV exhibits a Kondo resonance whose asymmetry is opposite to the experimentally observed one shown in Fig. 2(a). The asymmetry of dI/dV for $t_f = 0$ is a direct consequence of the particle-hole asymmetry of the conduction band. Indeed, reversing the latter via $\mu \rightarrow -\mu$, also leads to a reversal of the asymmetry in dI/dV , as shown by the dashed line in Fig. 3(a). Moreover, with increasing t_f/t_c , the height of the peak on the negative energy side, as well as the width of the dip in dI/dV , decrease while its minimum shifts to lower ener-

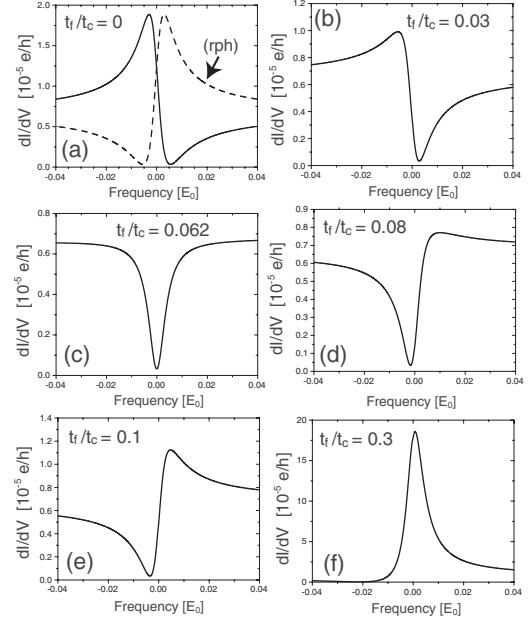


FIG. 3. (a)–(f) dI/dV at $\mathbf{r} = \mathbf{R}$ as a function of energy for $N = 2$, $N_t = 1.0/E_0$, $t_c = 0.001E_0$, and $J = 0.5E_0$ yielding $\varepsilon_f = 0.00520E_0$ and $s = 0.0847E_0$, and different values of t_f/t_c . The dashed line in (a) represents dI/dV for a conduction band with a reversed particle-hole (rph) asymmetry.

gies [Fig. 3(b)], leading to an almost symmetric dI/dV curve for $t_f/t_c = 0.062$ [Fig. 3(c)]. Increasing t_f/t_c even further [Fig. 3(d)] now reverses the asymmetry in dI/dV , yielding a peak on the positive energy side, and a minimum at slightly negative energies. The dI/dV line shape is now similar to that observed experimentally; however, the minimum in dI/dV is located at negative energies, thus clearly distinguishing the $N = 2$ and $N = 4$ cases. Further increasing t_f/t_c leads to an increase in the height of the peak and a widening of the dip [Fig. 3(f)].

We next turn to the discussion of the differential conductance in a Kondo lattice system, whose complex properties are determined by the competition between the Kondo screening of the magnetic moments and their antiferromagnetic ordering [2]. Its Hamiltonian is obtained by appropriately extending Eq. (1), and adding the term $\mathcal{H}_I = \sum_{\mathbf{r},\mathbf{r}'} I_{\mathbf{r},\mathbf{r}'} \mathbf{S}_{\mathbf{r}}^K \mathbf{S}_{\mathbf{r}'}^K$ representing the antiferromagnetic interaction between the moments. Here, we take $I_{\mathbf{r},\mathbf{r}'} > 0$ to be nonzero for nearest-neighbor sites only. Using again an Abrikosov pseudofermion representation of $\mathbf{S}_{\mathbf{r}}^K$, the Hamiltonian is decoupled by introducing the spatially uniform mean fields [20] $s = J \langle f_{\mathbf{r},\alpha}^\dagger c_{\mathbf{r},\alpha} \rangle$ and $\chi_0 = I \langle f_{\mathbf{r},\alpha}^\dagger f_{\mathbf{r},\alpha} \rangle$, where the latter is a measure of the magnetic correlations in the system. The constraint $\langle n_f \rangle = 1$ is enforced via an on-site energy, $\sum_{\mathbf{r}} \varepsilon_f f_{\mathbf{r},\alpha}^\dagger f_{\mathbf{r},\alpha}$. We then diagonalize the resulting mean-field Hamiltonian, and compute s , χ_0 , and ε_f self-consistently.

The magnetic interactions in the (screened) Kondo lattice have a profound effect on the form of the differential

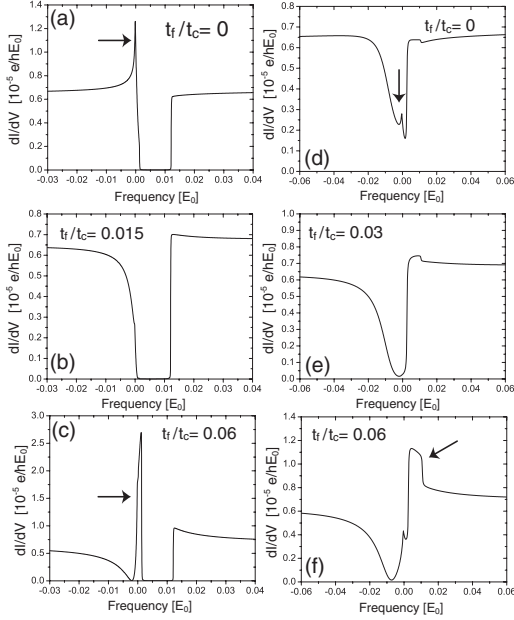


FIG. 4. Evolution of dI/dV in a Kondo lattice with t_f/t_c for $N = 2$, $N_t = 1/E_0$, $t_c = 0.001E_0$, $J = 0.5E_0$, and (a)–(c) $I/J = 0.001$ yielding $\varepsilon_f = 0.0012E_0$, $s = 0.0485E_0$, $\chi_0 = 0.00017E_0$, and (d)–(f) $I/J = 0.015$ yielding $\varepsilon_f = 0.00094E_0$, $s = 0.0480E_0$, and $\chi_0 = 0.00259E_0$.

conductance, as shown in Fig. 4, where we present the evolution of dI/dV with t_f/t_c for two different magnetic interaction strengths, $I/J = 0.001$ (left column) and $I/J = 0.015$ (right column). While for $I/J = 0.001$, dI/dV exhibits a hard hybridization gap for all values of t_f/t_c , only a suppression of the differential conductance around the Fermi energy is found for $I/J = 0.015$. However, in both cases, dI/dV exhibits a peak on the negative energy side [indicated by arrows in Figs. 4(a) and 4(d)], which arises from the van Hove singularity of the large (hybridized) Fermi surface. While this peak is suppressed with increasing t_f/t_c [Figs. 4(b) and 4(e)], a second peak emerges [indicated by arrows in Figs. 4(c) and 4(f)], which is the precursor of the emerging f -electron band. Increasing I/J leads to a shift of this peak to higher energies.

These results show that the existence of a two peak structure in dI/dV as predicted in Ref. [5] is not a generic feature of heavy-fermion materials. Rather, the specific form of dI/dV depends sensitively on t_f/t_c , the strength of the magnetic interaction, and the particle-hole asymmetry of the conduction band. In particular, the qualitative differences in dI/dV between $I/J = 0.001$ and 0.015 demonstrate that dI/dV is a direct measure for the strength of the antiferromagnetic interaction. Finally, we note that a theoretical analysis of the experimental dI/dV data by Schmidt *et al.* [1] on the heavy-fermion compound URu_2Si_2 , which is currently under way, will provide an important test for our model.

In summary, using a large- N theory, we showed that quantum interference between tunneling paths is crucial in explaining the experimentally observed Fano line shape in dI/dV . This allows one to uniquely extract the Kondo coupling, the ratio of the tunneling amplitudes, and the impurity spin from the experimental dI/dV curve. Finally, we showed that dI/dV reflects the strength of the antiferromagnetic interaction in Kondo lattice systems.

We would like to thank J. C. Davis, V. Madhavan, and H. Manoharan for stimulating discussions, and V. Madhavan for providing the data of Ref. [11]. D. K. M. would like to thank the James Franck Institute at the University of Chicago for its hospitality during various stages of this project. This work is supported by the U.S. Department of Energy under Grant No. DE-FG02-05ER46225.

-
- [1] A. R. Schmidt, M. H. Hamidian, P. Wahl, F. Meier, A. V. Balatsky, T. J. Williams, G. M. Luke, and J. C. Davis (to be published).
 - [2] S. Doniach, *Physica (Amsterdam)* **91B**, 231 (1977).
 - [3] M. B. Maple *et al.*, *J. Low Temp. Phys.* **99**, 223 (1995); A. Schroder *et al.*, *Nature (London)* **407**, 351 (2000); G. R. Stewart, *Rev. Mod. Phys.* **73**, 797 (2001); J. Custers *et al.*, *Nature (London)* **424**, 524 (2003); H. von Lohneysen *et al.*, *Rev. Mod. Phys.* **79**, 1015 (2007); P. Gegenwart, Q. Si, and F. Steglich, *Nature Phys.* **4**, 186 (2008).
 - [4] P. Coleman *et al.*, *J. Phys. Condens. Matter* **13**, R723 (2001); Q. M. Si *et al.*, *Nature (London)* **413**, 804 (2001); P. Sun and G. Kotliar, *Phys. Rev. Lett.* **91**, 037209 (2003); T. Senthil, S. Sachdev, and M. Vojta, *Phys. Rev. Lett.* **90**, 216403 (2003); I. Paul, C. Pepin, and M. R. Norman, *Phys. Rev. Lett.* **98**, 026402 (2007).
 - [5] M. Maltseva, M. Dzero, and P. Coleman, *Phys. Rev. Lett.* **103**, 206402 (2009).
 - [6] W. K. Park *et al.*, *Phys. Rev. Lett.* **100**, 177001 (2008).
 - [7] V. Madhavan *et al.*, *Science* **280**, 567 (1998).
 - [8] J. Li *et al.*, *Phys. Rev. Lett.* **80**, 2893 (1998).
 - [9] O. Ujsaghy *et al.*, *Phys. Rev. Lett.* **85**, 2557 (2000).
 - [10] N. Knorr *et al.*, *Phys. Rev. Lett.* **88**, 096804 (2002).
 - [11] V. Madhavan *et al.*, *Phys. Rev. B* **64**, 165412 (2001).
 - [12] H. C. Manoharan, C. P. Lutz, and D. M. Eigler, *Nature (London)* **403**, 512 (2000).
 - [13] A. A. Aligia and A. M. Lobos, *J. Phys. Condens. Matter* **17**, S1095 (2005).
 - [14] U. Fano, *Phys. Rev.* **124**, 1866 (1961).
 - [15] B. Coqblin and J. R. Schrieffer, *Phys. Rev.* **185**, 847 (1969).
 - [16] N. Read and D. M. Newns, *J. Phys. C* **16**, 3273 (1983).
 - [17] P. Coleman, *Phys. Rev. B* **28**, 5255 (1983).
 - [18] A. J. Millis and P. A. Lee, *Phys. Rev. B* **35**, 3394 (1987).
 - [19] N. E. Bickers, *Rev. Mod. Phys.* **59**, 845 (1987).
 - [20] T. Senthil, M. Vojta, and S. Sachdev, *Phys. Rev. B* **69**, 035111 (2004).
 - [21] E. Rossi and D. K. Morr, *Phys. Rev. Lett.* **97**, 236602 (2006).
 - [22] C. Caroli *et al.*, *J. Phys. C* **4**, 916 (1971).
 - [23] K. Schouteden, P. Lievens, and C. Van Haesendonck, *Phys. Rev. B* **79**, 195409 (2009).